

SIPL1 enhances the proliferation, attachment, and migration of CHO cells by inhibiting PTEN function

JASON DE MELO^{1,4}, VINCENT WU^{1,4}, LIZHI HE^{1,4}, JUDY YAN^{1,4} and DAMU TANG^{1,4}

¹Division of Nephrology, Department of Medicine, ²Division of Urology, Department of Surgery, McMaster University, ³Father Sean O'Sullivan Research Institute, ⁴The Hamilton Centre for Kidney Research (HCKR), St. Joseph's Hospital, Hamilton, ON L8N 4A6, Canada

Received May 1, 2014; Accepted June 13, 2014

DOI: 10.3892/ijmm.2014.1840

Abstract. The PTEN tumour suppressor plays critical roles in inhibiting cell proliferation, adhesion and migration through downregulation of the PI3K-AKT pathway. SIPL1 is a novel PTEN-negative regulator (PTEN-NR) that contributes to PTEN inactivation during tumorigenesis. However, whether SIPL1 plays a role in inhibiting PTEN function in the process of cell adhesion and migration remains unclear. The aim of this study was to investigate this possibility using CHO-K1 cells, and western blotting, qPCR analyses and microscopy. Results showed that the overexpression of SIPL1 in CHO-K1 cells decreased the amount of PTEN protein. The downregulation was not caused by an obvious reduction in PTEN mRNA levels or ubiquitin-dependent protein degradation. Nonetheless, the reduction was functional, as SIPL1 overexpression increased the activation of AKT under serum-starved conditions, promoting CHO-K1 cell proliferation in an AKT-dependent manner. Furthermore, SIPL1 increased the migration and attachment of CHO-K1 cells. Taken together, the evidence suggested that SIPL1 promotes AKT activation by decreasing the amount of PTEN protein in CHO-K1 cells, thereby promoting cell proliferation and migration.

Introduction

The phosphatase and tensin homolog deleted on chromosome 10 (PTEN; MMAC1) tumor suppressor was identified as a novel gene product commonly deleted in various types of cancer (1-3). PTEN is both a dual-specificity protein and lipid phosphatase (3,4), with PTEN suppressing tumorigenesis in its latter form. Mutations in the *PTEN* gene have been associated with various types of cancer (1,2,5-7), and are the causative

factor in Cowden syndrome (8,9). The homozygous deletion of the *PTEN* gene is embryonically lethal in mice (10).

PI3-kinase (PI3K) is an important enzyme in signal transduction. PI3K relays extracellular growth signals, which are derived from receptor tyrosine kinases, integrins and G-protein-coupled receptors, into intracellular signals. This is achieved by phosphorylating the second messenger lipid, phosphatidylinositol-4,5-bisphosphate (PIP₂) to phosphatidylinositol-3,4,5-triphosphate (PIP₃) (11). PIP₃ in turn recruits AKT to the plasma membrane, resulting in AKT activation. AKT subsequently regulates a number of downstream processes connected with cell survival and growth (12). PTEN exhibits lipid phosphatase activity (3,4), and dephosphorylates PIP₃ to PIP₂, thereby preventing the recruitment of AKT to the plasma membrane and downregulating AKT activation (12). PTEN also inhibits focal adhesion kinase (FAK) (13), a kinase that is activated by binding to integrins (14) and promotes cell migration, adhesion, spreading and angiogenesis (13,14). Thus, PTEN impedes various cell processes, including proliferation, cytoskeleton reorganization and angiogenesis.

Shank-interacting protein-like 1 (SIPL1; Sharpin) is a PTEN-negative regulator (PTEN-NR) that reduces PTEN-derived lipid-phosphatase activity through a direct association with PTEN (15). This decrease in PTEN function correlated with increased AKT activation and the promotion of tumorigenesis in *in vivo* xenograft models (15). Additionally, SIPL1 expression correlated with AKT activation and PTEN expression in primary cervical cancer (15). SIPL1 has been shown to play a key role in the activation of NF- κ B as part of the linear ubiquitin chain assembly complex (LUBAC) (16-18). As part of the LUBAC, SIPL1 promotes the formation of linear ubiquitin chains on NEMO, leading to the subsequent activation of NF- κ B and the promotion of cell survival. Additionally, SIPL1 is involved in the inside-out activation of β 1-integrin through direct binding to the α -integrin subunit (19). Loss of SIPL1 expression is also a causative factor of the chronic proliferative dermatitis (CPDM) phenotype in mice as a result of abnormal activation of NF- κ B (20-22).

In the present study, we examined the role of SIPL1 in the reduction of PTEN function in CHO-K1 cells with regard to cell proliferation, adhesion and migration. Ectopic SIPL1 decreased the PTEN protein, increased cell proliferation, and enhanced cell attachment and migration. Collectively, our

Correspondence to: Professor Damu Tang, The Hamilton Centre for Kidney Research (HCKR), T3310, St. Joseph's Hospital, 50 Charlton Avenue East, Hamilton, ON L8N 4A6, Canada
E-mail: damut@mcmaster.ca

Key words: SIPL1, PTEN, cell signalling, PI3 kinase, AKT

study supports the hypothesis that SIPL1 plays an important role in inhibiting PTEN function.

Materials and methods

Cell lines, plasmids and inhibitors. Human embryonic kidney 293T cells (HEK 293T) and Chinese hamster ovary K1 (CHO-K1; CHO) cells were purchased from the American Type Culture Collection (ATCC; Manassas, VA, USA), and cultured in Dulbecco's modified Eagle's medium (DMEM) (HEK 293T) or F-12 media (CHO-K1) supplemented with 10% fetal bovine serum (FBS; Sigma Aldrich, Oakville, ON, Canada) and 1% penicillin-streptomycin (Life Technologies, Burlington, ON, Canada). The pLHCX and pLHCX SIPL1 plasmids were constructed as previously described (13). AKT inhibitor VIII and the proteasomal inhibitor (MG132) were purchased from Calbiochem (EMD, Mississauga, ON, Canada) and Sigma Aldrich, respectively.

Retroviral overexpression of SIPL1. The overexpression of SIPL1 was carried out using a Gag-Pol (GP) and an envelope expressing vector (VSV-G) (Stratagene, Mississauga, ON, Canada). Briefly, the GP and VSV-G vectors were transiently co-transfected with pLHCX or pLHCX SIPL1 into HEK 293T cells using a calcium-phosphate procedure. The virus-containing medium was harvested 48 h later, filtered through a 0.45 μ M filter, and centrifuged at 20,000 x g for 120 min to concentrate the retrovirus. Following treatment with the virus, CHO-K1 cells were selected for stable integration with hygromycin (0.5 mg/ml; Sigma Aldrich).

Western blot analysis. Cell lysates were prepared in a buffer containing 20 mM Tris (pH 7.4), 150 mM NaCl, 1 mM EDTA, 1 mM EGTA, 1% Triton X-100, 25 mM sodium pyrophosphate, 1 mM NaF, 1 mM β -glycerophosphate, 0.1 mM sodium orthovanadate, 1 mM PMSF, 2 μ g/ml leupeptin and 10 μ g/ml aprotinin (Sigma Aldrich). Cell lysate (50 μ g) was separated on SDS-PAGE gels and transferred onto Amersham Hybond ECL nitrocellulose membranes (Amersham, Baie d'Urfe, QC, Canada). The membranes were blocked with 5% skim milk and incubated with the indicated antibodies at 4°C overnight. Appropriate HRP-conjugated secondary antibodies were incubated for 1 h at room temperature. Signals were detected using an ECL Western Blotting kit (Amersham). The primary and secondary antibodies used were: anti-Sharpin (1:1,000; Santa Cruz Biotechnology, Santa Cruz, CA, USA); anti-Sharpin (1:1,000; Abcam, Toronto, ON, Canada); anti-AKT (1:1,000; Santa Cruz Biotechnology); anti-AKT Ser473 phosphorylation (1:1,000; Cell Signaling Technology, Danvers, MA, USA); anti-GAPDH (1:5,000; Cell Signaling Technology), anti-actin (1:1,000; Santa Cruz Biotechnology), anti-goat (1:3,000; Santa Cruz Biotechnology), anti-mouse (1:3,000; GE Healthcare; Mississauga, ON, Canada) and anti-rabbit (1:3,000; GE Healthcare).

Real-time PCR analysis (RT-qPCR). Total RNA was isolated using TRIzol (Life Technologies). Reverse transcription was carried out using SuperScript III (Life Technologies) according to the manufacturer's instructions. Briefly, 2 μ g of RNA was converted to cDNA at 65°C for 6 min followed by 1-min

incubation on ice, 25°C for 11 min, 50°C for 60 min and 70°C for 15 min. qPCR primers used were: actin, forward: 5'-ACC GAG CGC GGC TAC AG-3' and reverse: 5'-CTT AAT GTC ACG CAC GAT TTC C-3'; PTEN, forward: 5'-TGT GGT CTG CCA GCT AAA GG-3' and reverse: 5'-CGG CTG AGG GAA CTC AAA GT-3' and SIPL1, forward: 5'-GCT ATT GCA GGT GGA GAC GA-3' and reverse: 5'-GCC TCC TGA AGC TGA ACA CT-3'. RT-qPCR was performed using the ABI 7500 Fast Real-Time PCR system in the presence of SYBR-Green according to the manufacturer's instructions (Applied Biosystems, Burlington, ON, Canada). Briefly, each reaction consisted of 1 μ l cDNA, 0.25 μ l forward primer (10 μ M), 0.25 μ l reverse primer (10 μ M), 4.75 μ l H₂O and 6.25 μ l of SYBR-Green Master Mix. The PCR reaction was carried out in a 96-well plate at 50°C for 2 min, 95°C for 10 min, followed by 40 cycles at 95°C for 15 sec and 60°C for 1 min. The samples were run in triplicate and repeated three times.

Serum stimulation. CHO-K1 cells (5×10^5) were seeded in a 6-well plate and incubated at 37°C overnight. The following day the cells were washed with PBS and incubated with serum-free F-12 media at 37°C overnight. The media were removed and replaced with complete F-12 media for 15, 30, 60, 120 or 180 min, followed by cell lysate collection and western blotting for AKT activation. It was determined that the parental CHO-K1 cells achieved maximum AKT activation at 30 min. CHO-K1 empty vector (EV) pLHCX or SIPL1 cells were seeded and serum-starved as described above. The media were then replaced with media containing 0, 2, 4, 6, 8 or 10% FBS and incubated at 37°C for 30 min followed by cell lysate collection.

Cell proliferation assay. A total of 500 CHO-K1 EV and SIPL1 cells were seeded in a 96-well plate and incubated at 37°C for 5 days. Proliferation was measured using the WST-1 cell proliferation assay kit (Millipore, Mississauga, ON, Canada) according to the manufacturer's instructions. Absorbance readings were measured with a plate reader (μ Quant; BioTek Instruments, Inc., Winooski, VT, USA) at 420 nm. For the treatment groups, the cells were treated with AKT inhibitor VIII to a final concentration of 2 μ M in the media or an equal volume of DMSO (Sigma Aldrich).

Wound healing assay. CHO-K1 EV of SIPL1 cells (1×10^5) were seeded in 6-well plates and incubated overnight at 37°C. Each well of the plate was scratched using a sterile pipette tip, both in the vertical and horizontal directions to generate the wound. The cells were washed with PBS to remove any dislodged cells and incubated at 37°C overnight. The plates were examined daily to observe the migration of the cell across the wound using a light microscope (Axiovert 200; Carl Zeiss, Jena, Germany).

Cell attachment. CHO-K1 EV of SIPL1 cells (2×10^5) were seeded in 6-well plates and incubated overnight at 37°C for 30, 60, 120 or 180 min, followed by removal of the unattached cells. The attached cells were released with trypsin (Life Technologies), and an aliquot of cells was removed and mixed with Trypan blue (Sigma Aldrich) to stain non-viable cells. The viable cells were counted under a light microscope (Axiovert 200; Carl Zeiss). The experiment was repeated in triplicate.

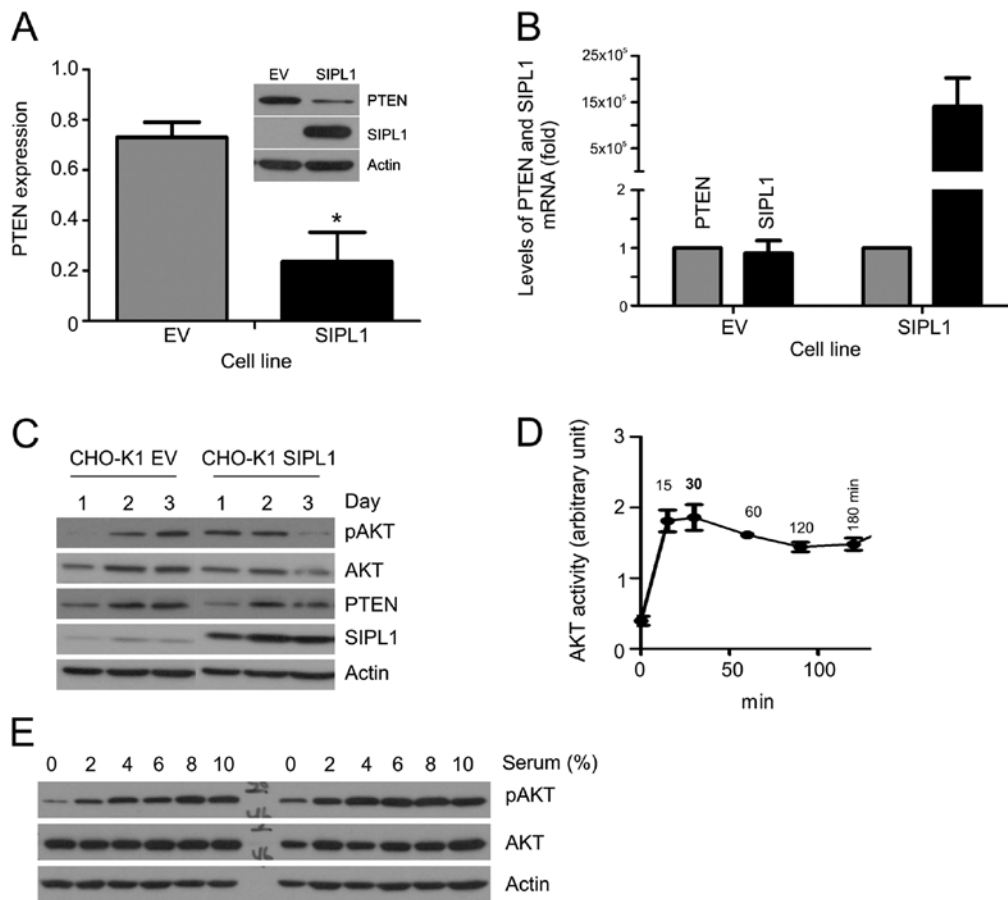


Figure 1. SIPL1 expression reduces PTEN function. (A) CHO-K1 cells were stably transfected with empty vector (EV) or SIPL1 followed by western blot analysis for the indicated proteins (inset). Experiments were repeated three times. PTEN was normalized to actin. Data are presented as means \pm standard error (SE). * $P < 0.05$ (two-tailed Student's t-test). (B) qPCR analysis of PTEN and SIPL1 in the indicated CHO-K1 cells. (C) The indicated CHO-K1 cells were seeded at a low density, followed by western blot analysis for the indicated proteins at day 1, 2 and 3 post-seeding. The analysis for the EV and SIPL1 cells was performed in the same gel and re-arranged for figure organization. (D) Serum-starved CHO-K1 cells were stimulated for a different period of time by 10% serum, and analyzed by western blot analysis for AKT, AKT activation (pAKT) and actin. AKT activation was normalized to total AKT and actin. Experiments were repeated three times. Data are presented as means \pm SE. (E) CHO-K1 EV and SIPL1 cells were serum-starved, stimulated with the indicated doses of serum for 30 min, and analyzed for the indicated proteins. Experiments were repeated three times. Typical images from a single repeat are shown.

Immunofluorescence. Immunofluorescence staining was performed by fixing cells with 4% paraformaldehyde for 20 min and permeabilized with 0.05% Triton X-100 for 15 min. One unit of Rodamine phalloidin was added to each slide at room temperature for 15 min according to the manufacturer's instructions. After washing, the slide was subsequently covered with VECTASHIELD mounting medium with DAPI (Vector Laboratories, Burlingame, CA, USA). Images were captured with a fluorescence microscope (Axiovert 200; Carl Zeiss).

Statistical analysis. Data are presented as means \pm standard error. Statistical analysis was performed using a Student's t-test or a two-way ANOVA. $P < 0.05$ was considered to indicate statistical significance.

Results

SIPL1 expression facilitates AKT activation. The human SIPL1 cDNA was stably expressed into CHO-K1 cells using a retrovirus (Fig. 1A). SIPL1 overexpression resulted in a marked decrease of the PTEN protein (Fig. 1A). To determine whether the decreased PTEN protein was associated

with reduction in PTEN mRNA abundance, we quantified the PTEN mRNA in CHO-K1 empty vector (EV) and SIPL1 cells. As expected, the overexpression of SIPL1 in CHO-K1 SIPL1 cells was readily demonstrated (Fig. 1B). However, in comparison to CHO-K1 EV cells, comparable levels of PTEN mRNA were detected in CHO-K1 SIPL1 cells (Fig. 1B). It, thus, seems unlikely that SIPL1 reduces the PTEN protein by reducing PTEN mRNA.

PTEN downregulation results in the elevation of AKT activation. To examine the activation of AKT, we seeded CHO-K1 EV and SIPL1 cells at comparable densities followed by the examination of AKT phosphorylation at serine 473 (pAKT Ser473), a well-established surrogate marker of AKT activation (12). During the course of three days, an increase in pAKT Ser473 was detected in CHO-K1 SIPL1 cells in comparison to CHO-K1 EV cells at day 1, at the time when cells were largely sub-confluent (Fig. 1C), while the increase was not clear on days 2 and 3, when the cell density was significantly higher (Fig. 1C). The density-dependent AKT activation observed in CHO-K1 SIPL1 cells matched with the levels of PTEN protein in the respective cell densities, where on day 1 PTEN CHO-K1 EV cells were higher than those of PTEN CHO-K1 SIPL1

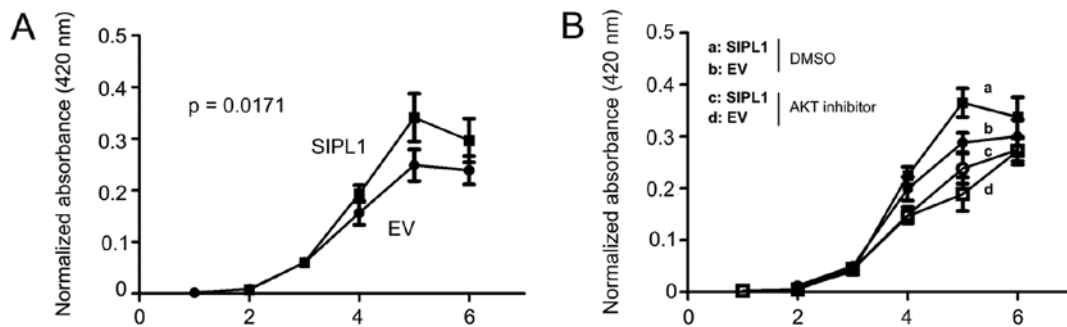


Figure 2. SIPL1 enhances CHO-K1 cell proliferation in an AKT-dependent manner. (A) CHO-K1 EV and SIPL1 cells were seeded in 96-well (500 cells/well) plates, followed by determination of the cell number using WST assay. Experiments were repeated three times. Data are presented as means \pm SE. (B) Statistical analysis was performed using a two-way ANOVA. The proliferation rates of CHO-K1 EV and SIPL1 cells were determined in the presence of DMSO or an AKT inhibitor. Experiments were repeated three times. Data are presented as means \pm SE. Statistical analysis was performed using a two-way ANOVA for the following comparisons: curve a vs. b ($P < 0.05$), curve a vs. c ($P < 0.01$), curve b vs. d ($P < 0.01$), and curve c vs. d ($P = 0.177$).

cells. Of note, the difference was eradicated in the respective day 2 and 3 cells (Fig. 1C).

To examine SIPL1-facilitated AKT activation, CHO-K1 EV and SIPL1 cells were examined for serum-induced AKT activation. Prior to this task, the kinetics of serum-induced AKT activation were determined. The addition of a medium containing 10% serum to serum-starved CHO-K1 cells resulted in peak AKT activation at 30 min (Fig. 1D). With the kinetics determined, we treated serum-starved CHO-K1 EV and SIPL1 cells with different doses of serum, and examined the peak-AKT activation. In comparison to CHO-K1 EV cells, CHO-K1 SIPL1 cells maintained higher levels of pAKT Ser473 even under serum-free conditions (Fig. 1E). Thus, the above observations support that SIPL1-mediated downregulation of PTEN in CHO-K1 cells facilitates AKT activation.

SIPL1 enhances CHO-K1 cell proliferation. AKT activation promotes cell proliferation (21). To examine whether facilitation of AKT activation of SIPL1 would enhance CHO-K1 cell proliferation, CHO-K1 EV and SIPL1 cells were seeded in 96-well plates and their growth was monitored over a course of six days using a WST assay. SIPL1 cells proliferated significantly more rapidly as compared to EV cells (Fig. 2A). The increase in CHO-K1 SIPL1 cell proliferation over CHO-K1 EV cells was only observed within a certain time frame (Fig. 2A), an observation that is in concordance with SIPL1-facilitating AKT activation in these cells in a density-dependent manner (Fig. 1C). To consolidate the contributions of AKT activation to the SIPL1-enhanced proliferation of CHO-K1 cells, CHO-K1 EV and SIPL1 cells were treated with an inhibitor of AKT, AKT inhibitor VIII. We have previously demonstrated that the AKT inhibitor VIII potently inhibited AKT activation (24,25). As expected, CHO-K1 SIPL1 cells proliferated at a faster rate compared to CHO-K1 EV cells in the vehicle (DMSO) treatment group (Fig. 2B). Inhibition of AKT activation significantly reduced the proliferation of CHO-K1 EV and SIPL1 cells (Fig. 2B). Of note, there was no significant difference between SIPL1-expressing cells and EV cells treated with the AKT inhibitor (Fig. 2B). Taken together, the above results demonstrate a critical role of AKT activation in SIPL1-accelerated CHO-K1 cell proliferation.

SIPL1 expression increases the attachment and spread of CHO-K1 cells. SIPL1 facilitates AKT activation, particularly at lower densities (Fig. 1C). Additionally, SIPL1 enhances CHO-K1 cell proliferation in an AKT activity-dependent manner (Fig. 2B). These observations suggest that the property of cell adhesion may be altered in SIPL1-overexpressing cells. This possibility is in concordance with the importance of cell adhesion to cell proliferation (26). To examine the effect of SIPL1 expression on cell attachment, CHO-K1 EV and SIPL1 cells were seeded in culture dishes at comparable densities and allowed to adhere for 30-180 min. At each time-point, any unattached cells were removed, and the remaining cells were trypsinized and counted using a haemocytometer. CHO-K1 SIPL1 cells were able to attach to the culture dish at a significantly higher rate compared to CHO-K1 EV cells (Fig. 3A).

As cytoskeleton reorganization is essential for cell attachment, we examined the formation of actin fibres in both CHO-K1 EV and SIPL1 cells. While actin stress fibres were clearly visible 3 h after attachment for CHO-K1 SIPL1 cells, they were not clearly present in CHO-K1 EV cells (Fig. 3B). When quantified, 79.9% of SIPL1-expressing cells and 42.5% of EV cells were able to form defined actin cytoskeletons within 3 h (Fig. 3C). At the 24-h time-point, there were no differences between actin stress fibres formed between CHO-K1 EV and SIPL1 cells (Fig. 3B and C). This suggests an increase in the rate at which SIPL1-expressing cells spread and form defined actin cytoskeletons (Fig. 3B and C). Taken together, we have demonstrated that SIPL1 enhances cell attachment by increasing the kinetics of forming actin stress fibres.

SIPL1 promotes the motility of CHO-K1 cells. The dynamics of cytoskeleton organization affects the migration ability of a cell. By facilitating the rapid formation of actin stress fibres, SIPL1 may also play a role in cell motility. To investigate this possibility, a wound healing assay was performed on CHO-K1 EV and SIPL1 cells. A 'wound' was created by making a scratch across the culture dish followed by monitoring the rate of gap-closing. At day 1 and 2 post-scratching, CHO-K1 SIPL1 cells closed the gaps with faster kinetics compared to the CHO-K1 EV cells (Fig. 4).

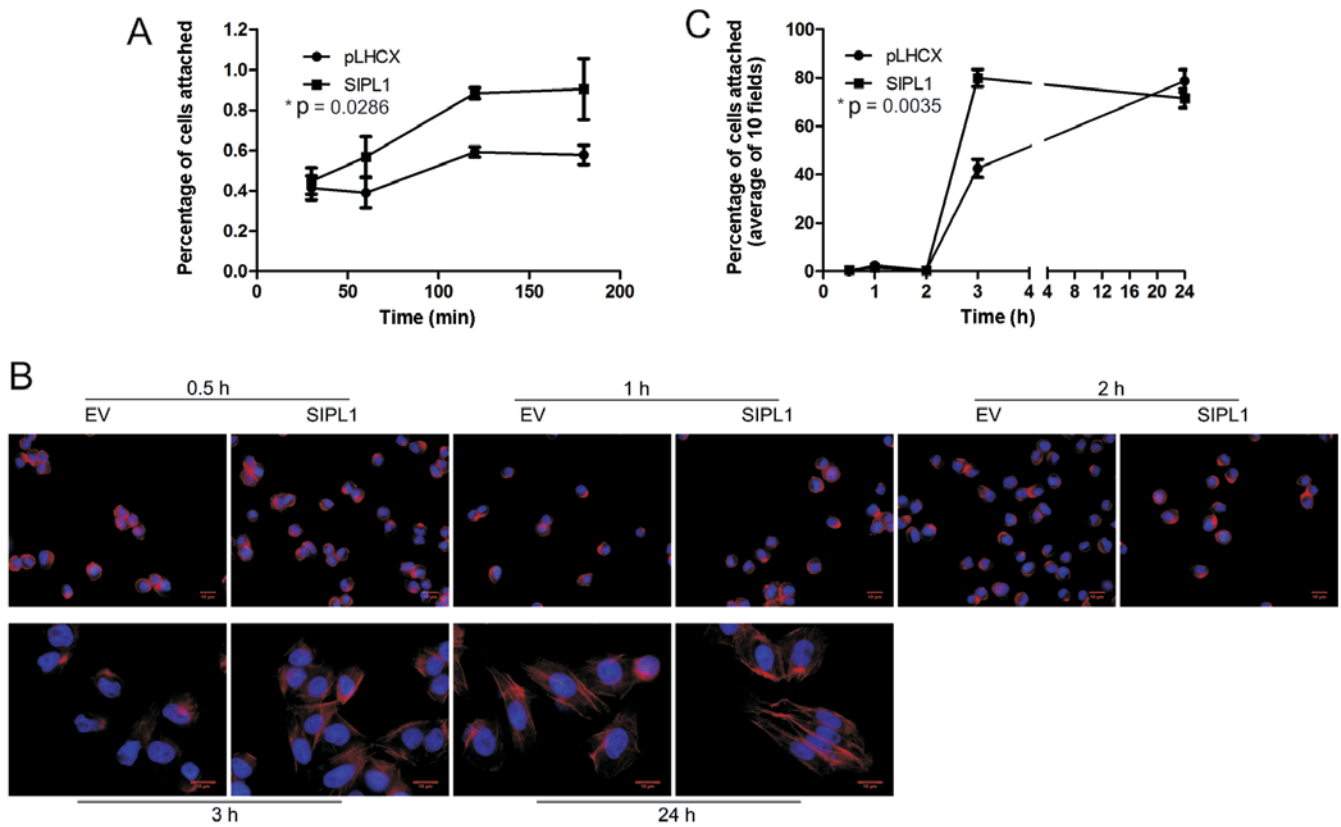


Figure 3. SIPL1 promotes CHO-K1 cell adhesion. (A) CHO-K1 EV and SIPL1 cells (2×10^5) were seeded for 0.5, 1, 2, 4 and 24 h. The number of adhered cells at individual time-points was counted. Experiments were repeated three times. Data are presented as means \pm SE. Statistical analysis was performed using two-way ANOVA. (B and C) CHO-K1 EV and SIPL1 cells were seeded in chamber slides for the indicated time points, followed by staining for actin stress fiber using Rodamine phalloidin. Ten separate fields of cells were quantified visually for the formation of actin fibres. (B) Typical images and (C) quantification of actin stress fiber-positive cells are shown. Statistical analysis was performed using a two-way ANOVA.

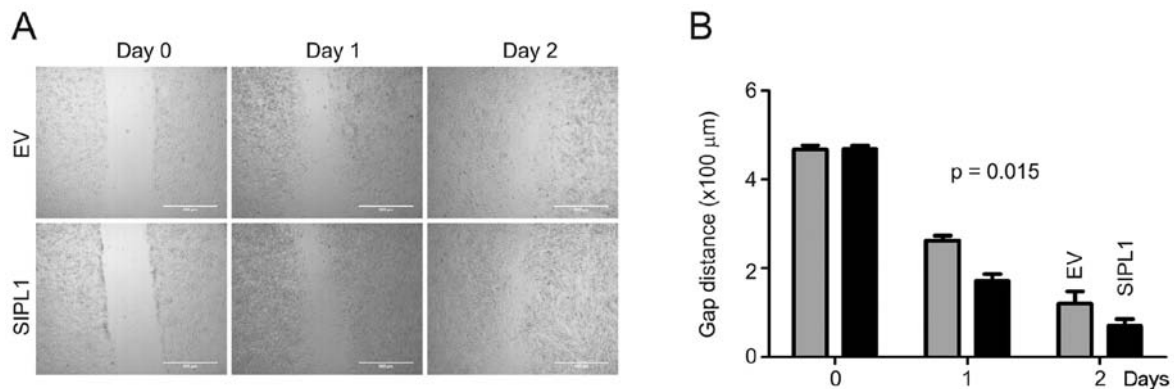


Figure 4. SIPL1 increases the motility of CHO-K1 cells. A 'wound' was created in the CHO-K1 EV and SIPL1 cells, and the wound closure was monitored daily. Experiments were repeated three times. (A) Typical images and (B) quantification are shown. Statistical analysis was performed using two-way ANOVA.

Discussion

To examine the impact of SIPL1 on PTEN activity, SIPL1 was overexpressed in CHO-K1 cells. CHO-K1 cells were selected for a number of reasons: SIPL1 expression in CHO-K1 cells had previously been shown to increase their tumorigenic potential (27); SIPL1 is highly expressed in ovary tissues (27); and CHO-K1 cells are commonly used to express ectopic proteins (28). Overexpression of SIPL1 resulted in a marked decrease in the amount of PTEN protein (Fig. 1A). NEDD4-1

has been shown to poly-ubiquitinate PTEN and reduces the amount of PTEN present in the cell lysate. This reduction is reversed following treatment with MG132 (29), a potent inhibitor of the proteasome (30). It was postulated that the SIPL1 protein may also promote the degradation of PTEN via the proteasome. Recently, SIPL1 was shown to form part of the LUBAC, a complex of proteins that form linear ubiquitin chains on NF- κ B and promotes its activity (16-18). The SIPL1 protein also possesses a ubiquitin-like (UBL) domain and a NFZ domain required for its binding to ubiquitin (15,18), lending

credence to this possibility. However, we were unable to detect any effect of MG132 on the SIPL1-induced reduction of the PTEN protein in CHO-K1 cells (data not shown), suggesting that the ubiquitin proteasome system may not be significant in SIPL1-induced downregulation of the PTEN protein. As SIPL1-overexpressing CHO-K1 cells did not exhibit reduction in PTEN mRNA (Fig. 1B), it is possible that a mechanism independent of the protease system and mRNA abundance may be involved in SIPL1-induced reduction of the PTEN protein.

Previous studies have concluded that SIPL1 promotes the activation of AKT through the direct binding to and inactivation of PTEN (15). Results of the present study show that by reducing the cellular PTEN protein concentration, SIPL1 was able to elevate AKT activation and induce CHO cell proliferation in an AKT-dependent manner. AKT activity is critical in a number of cell processes including cell proliferation, cell adhesion, migration and cytoskeleton reorganization (31). While we have shown that AKT activity is critical for SIPL1-enhanced CHO-K1 cell proliferation, whether AKT is also critical in CHO-K1 cell adhesion and migration remains unclear, owing to the essential role of FAK in cell adhesion and migration. Future studies should therefore address the impact of SIPL1 on FAK function.

SIPL1 promotes the activation of NF- κ B (16-18) through its association with the LUBAC. NF- κ B can have a direct impact on PTEN expression by binding the promoter region of PTEN, thereby repressing its transcription (32). Results of this study show that reduction in the PTEN protein was not due to changes in the proteasomal degradation or mRNA transcription of PTEN, indicating the SIPL1 regulation of PTEN may be independent of its NF- κ B activating activity as part of the LUBAC.

SIPL1 expression appears to regulate PTEN at a greater extent at lower cell densities. This is in agreement with our observations that SIPL1 facilitated cell migration and adhesion concomitantly with enhancing the formation of the actin stress fibres. This is in agreement with previous studies indicating that the overexpression of PTEN impaired cell migration, spreading and attachment (33,34). High cell densities have been shown to promote a mild hypoxic condition in cell cultures (35), a process in which the PI3K/AKT pathway induces changes in gene expression through its effects on HIF1 α and Redd1 and promotes cell survival (35). While SIPL1 may be able to inhibit PTEN to a greater extent at lower cell densities, its role in inactivating PTEN may become reduced at high densities, where the PI3K/AKT pathway may overpower PTEN function. In addition to regulating PTEN, and participating in the LUBAC to regulate NF- κ B signaling, SIPL1 has also been shown to inhibit β 1-integrin activation (19). This is contrary to our understanding of activities of SIPL1. The differences may be attributable to different assay conditions.

Taken together, the present study has shown that SIPL1 plays a role in the reduction of PTEN, leading to AKT activation. AKT activity enhances CHO-K1 cell proliferation, and may also contribute to increased cell attachments and motility. Although it is suspected that SIPL1 induces PTEN reduction independently of its role in NF- κ B activation, this possibility cannot be excluded. Furthermore, the ability of SIPL1 to promote FAK activation via PTEN inactivation should be investigated in the future.

Acknowledgements

The present study was supported by the Canadian Institute of Health Research (CIHR) grant (COP-107971) to D.T.

References

1. Steck PA, Pershouse MA, Jasser SA, *et al*: Identification of a candidate tumour suppressor gene, *MMAC1*, at chromosome 10q23.3 that is mutated in multiple advanced cancers. *Nat Genet* 15: 356-362, 1997.
2. Li J, Yen C, Liaw D, *et al*: PTEN, a putative protein tyrosine phosphatase gene mutated in human brain, breast, and prostate cancer. *Science* 275: 1943-1947, 1997.
3. Myers MP, Stolarov JP, Eng C, *et al*: P-TEN, the tumor suppressor from human chromosome 10q23, is a dual-specificity phosphatase. *Proc Natl Acad Sci USA* 94: 9052-9057, 1997.
4. Maehama T and Dixon JE: The tumor suppressor, PTEN/MMAC1, dephosphorylates the lipid second messenger, phosphatidylinositol 3,4,5-trisphosphate. *J Biol Chem* 273: 13375-13378, 1998.
5. Li DM and Sun H: PTEN/MMAC1/TEP1 suppresses the tumorigenicity and induces G₁ cell cycle arrest in human glioblastoma cells. *Proc Natl Acad Sci USA* 95: 15406-15411, 1998.
6. Robertson GP, Furnari FB, Miele ME, *et al*: In vitro loss of heterozygosity targets the *PTEN/MMAC1* gene in melanoma. *Proc Natl Acad Sci USA* 95: 9418-9423, 1998.
7. Duerr EM, Rollbrocker B, Hayashi Y, *et al*: PTEN mutations in gliomas and glioneuronal tumors. *Oncogene* 16: 2259-2264, 1998.
8. Mallory SB: Cowden syndrome (multiple hamartoma syndrome). *Dermatol Clin* 13: 27-31, 1995.
9. Liaw D, Marsh DJ, Li J, *et al*: Germline mutations of the *PTEN* gene in Cowden disease, an inherited breast and thyroid cancer syndrome. *Nat Genet* 16: 64-67, 1997.
10. Di Cristofano A, Pesce B, Cordon-Cardo C, Pandolfi PP, Cristofano AD and PP: Pten is essential for embryonic development and tumour suppression. *Nat Genet* 19: 348-355, 1998.
11. Yuan TL and Cantley LC: PI3K pathway alterations in cancer: variations on a theme. *Oncogene* 27: 5497-5510, 2008.
12. Stambolic V, Suzuki A, Mirtsos C, *et al*: Negative regulation of PKB/Akt-dependent cell survival by the tumor suppressor PTEN. *Cell* 95: 29-39, 1998.
13. Tamura M, Gu J, Matsumoto K, Aota S, Parsons R and Yamada KM: Inhibition of cell migration, spreading, and focal adhesions by tumor suppressor PTEN. *Science* 280: 1614-1617, 1998.
14. Zhao X and Guan JL: Focal adhesion kinase and its signaling pathways in cell migration and angiogenesis. *Adv Drug Deliv Rev* 63: 610-615, 2011.
15. He L, Ingram A, Rybak AP and Tang D: Shank-interacting protein-like 1 promotes tumorigenesis via PTEN inhibition in human tumor cells. *J Clin Invest* 120: 2094-2108, 2010.
16. Gerlach B, Cordier SM, Schmukle AC, *et al*: Linear ubiquitination prevents inflammation and regulates immune signalling. *Nature* 471: 591-596, 2011.
17. Tokunaga F, Nakagawa T, Nakahara M, *et al*: SHARPIN is a component of the NF- κ B-activating linear ubiquitin chain assembly complex. *Nature* 471: 633-636, 2011.
18. Ikeda F, Deribe YL, Skånland SS, *et al*: SHARPIN forms a linear ubiquitin ligase complex regulating NF- κ B activity and apoptosis. *Nature* 471: 637-641, 2011.
19. Rantala JK, Pouwels J, Pellinen T, *et al*: SHARPIN is an endogenous inhibitor of β 1-integrin activation. *Nat Cell Biol* 13: 1315-1324, 2011.
20. Liang Y: Chronic proliferative dermatitis in mice: NF κ B activation/inflammatory disease. *Patholog Res Int* 2011: 936794, 2011.
21. Gijbels MJ, Hogenesch H, Blauw B, Roholl P and Zurcher C: Ultrastructure of epidermis of mice with chronic proliferative dermatitis. *Ultrastruct Pathol* 19: 107-111, 1995.
22. Seymour RE, Hasham MG, Cox GA, Shultz LD, Hogenesch H, Roopenian DC and Sundberg JP: Spontaneous mutations in the mouse Sharpin gene result in multiorgan inflammation, immune system dysregulation and dermatitis. *Genes Immun*: 416-421, 2007.

23. Manning BD and Cantley LC: AKT/PKB signaling: navigating downstream. *Cell* 129: 1261-1274, 2007.
24. Xie Y, Yan J, Cutz JC, *et al*: IQGAP2, A candidate tumour suppressor of prostate tumorigenesis. *Biochim Biophys Acta* 1822: 875-884, 2012.
25. Yan J, Wong N, Hung C, Chen WX and Tang D: Contactin-1 reduces E-cadherin expression via activating AKT in lung cancer. *PLoS One* 8: e65463, 2013.
26. Gilmore AP and Romer LH: Inhibition of focal adhesion kinase (FAK) signaling in focal adhesions decreases cell motility and proliferation. *Mol Biol Cell* 7: 1209-1224, 1996.
27. Jung J, Kim JM, Park B, *et al*: Newly identified tumor-associated role of human Sharpin. *Mol Cell Biochem* 340: 161-167, 2010.
28. Greene G, Gilna P, Waterfield M, Baker A, Hort Y and Shine J: Sequence and expression of human estrogen receptor complementary DNA. *Science* 231: 1150-1154, 1986.
29. Wang X, Trotman LC, Koppie T, *et al*: NEDD4-1 is a proto-oncogenic ubiquitin ligase for PTEN. *Cell* 128: 129-139, 2007.
30. Zanutto-Filho A, Braganhol E, Battastini AM and Moreira JC: Proteasome inhibitor MG132 induces selective apoptosis in glioblastoma cells through inhibition of PI3K/Akt and NFkappaB pathways, mitochondrial dysfunction, and activation of p38-JNK1/2 signaling. *Invest New Drugs* 30: 2252-2262, 2012.
31. Vivanco I and Sawyers CL: The phosphatidylinositol 3-Kinase AKT pathway in human cancer. *Nat Rev Cancer* 2: 489-501, 2002.
32. Ghosh-Choudhury N, Mandal CC, Ghosh-Choudhury N and Ghosh Choudhury G: Simvastatin induces derepression of PTEN expression via NFkB to inhibit breast cancer cell growth. *Cell Signal* 22: 749-758, 2010.
33. Attwell S, Mills J, Troussard A, Wu C and Dedhar S: Integration of cell attachment, cytoskeletal localization, and signaling by integrin-linked kinase (ILK), CH-ILKBP, and the tumor suppressor PTEN. *Mol Biol Cell* 14: 4813-4825, 2003.
34. Mondal S, Subramanian KK, Sakai J, Bajrami B and Luo HR: Phosphoinositide lipid phosphatase SHIP1 and PTEN coordinate to regulate cell migration and adhesion. *Mol Biol Cell* 23: 1219-1230, 2012.
35. Jin HO, An S, Lee HC, *et al*: Hypoxic condition- and high cell density-induced expression of Redd1 is regulated by activation of hypoxia-inducible factor-1 α and Sp1 through the phosphatidylinositol 3-kinase/Akt signaling pathway. *Cell Signal* 19: 1393-1403, 2007.